Available online at www.sciencedirect.com
SCIENCE DIRECT®
ELSEVIER
Journal of Magnetism and Magnetic Materials 261 (2003) 21–28
journal of magnetism and magnetic materials
www.elsevier.com/locate/jmmm

# Magnetic relaxation of diluted and self-assembled cobalt nanocrystals

X.X. Zhang[a,*], G.H. Wen[a], Gang Xiao[b], Shouheng Sun[c]

[a] *Department of Physics, Hong Kong University of Science and Technology, Clear Water Bay, Kowloon, Hong Kong, China*
[b] *Physics Department, Brown University, Providence, RI 02912, USA*
[c] *IBM T. J. Watson Research Center, Yorktown Heights, New York 10598, USA*

Received 8 August 2002; received in revised form 15 October 2002

**Abstract**

We have studied the magnetic relaxation of monodispersed 4 nm cubic ε-cobalt nanocrystals in both randomly oriented and pre-aligned assemblies. The blocking temperature $T_B$, for the closely packed Co nanocrystal assemblies, is 30% higher than that of the highly diluted and well-dispersed Co nanocrystal-organic composites. This increase is attributed to the strong magnetic dipole interaction induced from the close packing of the nanocrystals. It is found that the frequency-dependent susceptibility data, obtained from the diluted samples, can be fitted to the half-circle Argand Diagrams, indicating a single barrier (or very narrow energy distribution) of the nanocrystals. This agrees well with the physical observation from TEM that the nanocrystals are monodispersed. The long time magnetic relaxation measurements reveal that energy barrier distribution in a pre-aligned nanocrystal assembly is significantly different from that in a randomly oriented one.


*PACS:* 75.50.Tt; 75.60.Lr; 75.75.+a; 75.40.Gb

*Keywords:* Monodispersed nanoparticles; Magnetic relaxation; Magnetic dipole interaction

Controlled self-assembly of monodispersed magnetic nanocrystals (ncs) has shown great potential in fabricating functional magnetoelectronic nanodevices [1,2] and ultra-high density magnetic recording media [3,4]. In a self-assembled NC array, NC size, shape, interparticle spacing, and coating can have important effects on the assembly structure and the physical properties of the NCs in an assembly [5–10]. We are interested in the well-controlled single domain magnetic NC assemblies, because important magnetic relaxation information of the NCs can be extracted from the magnetic properties of these assemblies. In the past, irregular shapes and large size distribution often impeded the observation of the intrinsic magnetic relaxation phenomena [5,6,11–13]. On the contrary, magnetic NCs with uniform shape and narrow size distribution can offer an ideal model system to test the physics of magnetic relaxation in single-domain NC assemblies. Such

*Corresponding author. Tel.: +852-2358-7493; fax: +852-2358-1652.
*E-mail address:* phxxz@ust.hk (X.X. Zhang).

0304-8853/03/$ - see front matter 
PII: S0304-8853(02)01408-7

basic magnetic understanding will also favor future fabrication of highly efficient magneto-nanoelectronic devices.

The monodispersed cobalt NCs were synthesized in solution phase via superhydride reduction of cobalt chloride in the presence of trialkylphosphine and oleic acid [15]. The NCs have a cubic structure, are encapsulated by the oleic acid and can be dispersed readily in hexane or other non-polar solvents. Spherical in shape, these NCs behave like isolated and independent single-domain magnetic units in the solution phase. Once dried, they can solidify into 2D or 3D magnetic superlattices. Using the Quantum Design SQUID magnetometer, we measured the magnetic properties of three NC samples (particle size of 4 nm). Two liquid phase (diluted) samples were cooled from room temperature at which both samples were liquid to 5 K where the sample were frozen to solid in zero and 5 T magnetic field. To avoid the dipole–dipole interaction and to have a signal large enough for the magnetic measurements, we prepared a magnetic fluid using hexane with a NC volume concentration of $\sim 0.3$ vol%. The Co NCs had a random distribution of magnetic easy axis (referred to as Sample Random) in zero field cooling and aligned easy axes (Sample Aligned) in a 5 T field cooling. Fluid of 0.1 ml was sealed in Teflon cage and cooled to 5 K in a zero magnetic field, then we made a solid sample. In this sample, the easy axes of the NCs randomly distributed. Before we finished the measurement, this sample was always kept at solid state. This sample is referred as Sample Random. After all the measurement on the Sample Random was finished, the sample was heated to room temperature and melted into liquid completely. The sample was cooled again to 5 K in a 5 T magnetic field, by which the easy axes of the NCs were aligned and fixed in the field direction. Again, the aligned sample (referred as Sample aligned) was always kept in solid state before the finishing all the measurements. As a comparison to these two diluted samples, we also prepared a third sample composed of a self-assembled array of Co NCs (Sample Array) by depositing the hexane dispersion of the Co NCs on a silicon (1 0 0) substrate via slow evaporation of the hexane at room temperature. In this self-assembled NC array, interparticle spacing is only about 4–5 nm [15] and strong magnetic dipole interaction is expected.

We have measured the temperature dependent magnetic susceptibility in these three samples, as shown in Fig. 1. The blocking phenomenon is clearly seen in the zero-field-cooled and field-cooled processes. While the blocking temperature $T_B$ is $\sim 31.5$ K and $\sim 33.5$ K for the Sample Random and Aligned, respectively, $T_B$ increases to 40 K in the Sample Array. In other words, the close packed NCs yield a $T_B \sim 30\%$ higher over that of diluted ones. This increase of the blocking temperature is likely due to the larger dipolar interaction existing in the array [5–7] since the only difference between the Sample Array and Sample Random or Aligned is the packing density. This observation is consistent with a Monte Carlo simulation on randomly distributed ultrafine particles [7]. Assuming that the dominant cause is the emerging dipolar interaction, the simulation shows an increasing $T_B$ as particle concentration increases.

Our analysis shows that, above $T_B$, the susceptibility is well described by the Curie–Weiss law $\chi(T) = C/(T - \theta)$. The Curie–Weiss temperature is small ($\theta \cong -5.2$ K) for the diluted nanocrystals (in Sample Random and Aligned). However for the arrayed NCs, $\theta$ increases to $\cong -8.5$ K, again a result of the larger dipolar interaction. The increasingly negative $\theta$ at higher particle

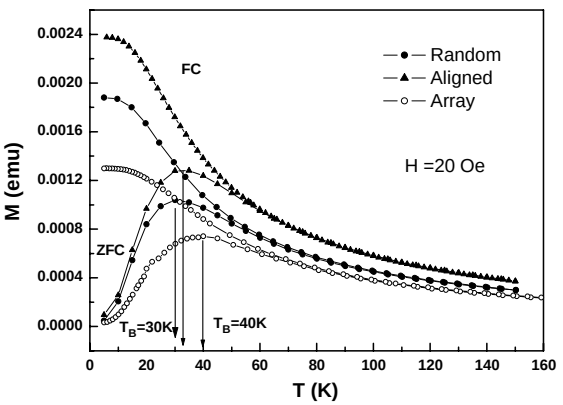


Fig. 1. Temperature-dependent magnetization obtained in the zero-field-cooled and field-cooled processes for Sample Random and Sample Applied.

concentrations was also predicted in the same Monte Carlo simulation where the role of dipolar interaction is assumed.

The temperature-dependent AC susceptibility measured at different frequencies is commonly used for obtaining the energy barrier in the single-domain particles. The AC susceptibility is given as [14]

$$\chi(\omega) = \chi'(\omega) - i\chi(\omega). \tag{1}$$

The in-phase (real part) susceptibility $\chi'$and the out-phase (imaginary part) susceptibility $\chi''$are related by the following equations:

$$\chi' = \chi_s + \frac{\chi_T - \chi_s}{1 + (\omega\tau)^2}, \tag{2a}$$

$$\chi'' = \omega\tau\left(\frac{\chi_T - \chi_s}{1 + (\omega\tau)^2}\right), \tag{2b}$$

where $\tau$ is the relaxation time given by $\tau = 1/\Gamma = \nu^{-1}\exp(U/k_BT)$, $\chi_T$ is the isothermal susceptibility in the limit $\omega\to 0$ (or DC thermal equilibrium susceptibility), and $\chi_s$ is the adiabatic susceptibility in the limit $\omega\to\infty$ (or very high frequency). It is well known that when $\omega\tau = 1$, $\chi''$ shows a maximum according to relation (2b). For a given temperature ($T$), this maximum provides the relaxation time $\tau(T)$ [14].

For a single domain particle, from low temperatures (the blocked state) to high temperatures (the superparamagnetic state), the relaxation time $\tau$ changes from a very large number to a very small one. Therefore, for a given $\omega$ ($=2\pi f$), $\omega\tau$ will decrease from $\sim\infty$ (at very low $T$) to $\sim 0$ (at very high $T$), consequently, both $\chi'(T)$ and $\chi''(T)$ will show a maximum. A peak appears in $\chi''(T)$ at $\omega\tau = 1$, i.e.

$$\omega[\nu^{-1}\exp(U/k_BT_p)] = 1, \tag{3}$$

where $T_p$ denotes the peak temperature in $\chi''(T)$. With the change of the frequency, $T_p$ will shift accordingly, and Eq. (3) is often used to extract the value of energy barrier, $U$, and the attempt frequency $\nu$, by plotting the frequency against $T_p$ using the following equation derived from Eq. (3):

$$\ln 2\pi f = \ln(\nu) - \frac{U}{k_BT_P}. \tag{4}$$

Fig. 2 shows the $\chi'(T)$ and $\chi''(T)$ data at different frequencies for the Sample Random. It shows, with increasing frequency, the peaks in both $\chi'(T)$ and $\chi''(T)$ shifting to higher temperatures. Our analysis showed that $T_p$ in $\chi''(T)$ vs. frequency follows Eq. (4) very well, with $\nu = 1.0\times 10^{14}\,s^{-1}$ and $U/k_B = 733\pm 6$ K. The extracted energy barrier corresponds to an anisotropy constant $K = 3.02\times 10^5\,J/m^3$ for our 4 nm particles, which is consistent with the $K = 1.87\times 10^5$ and $3.08\times 10^5\,J/m^3$ for 5 and 3 nm cubic Co particles [9]. The latter anisotropy constants were obtained by measuring the temperature induced spontaneous magnetic noise of self-assembled lattices of uniformed superparamagnetic nanoparticles. Some other values of $K$ for cubic Co have also been reported, for example, $2.7\times 10^5\,J/m^3$ [16], $1.2\times 10^5\,J/m^3$ [17] and $5\times 10^5\,J/m^3$ to $3\times 10^6\,J/m^3$ [18]. Thus, our $K$

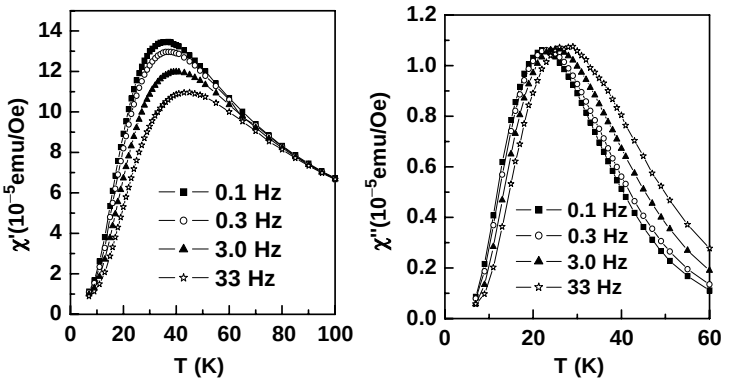


Fig. 2. Temperature dependent magnetic susceptibility obtained on Sample Random.

value is in general agreement with the earlier reported values.

We note that the fitted value of attempt frequency, $v = 1.0 \times 10^{14}\,s^{-1}$, is significantly larger than reported values [19–22]. As a comparison, the atomic spin flip rate, $v_s$, is on the order of $10^{13}\,s^{-1}$. Obviously, the attempt frequency cannot be larger than $v_s$. This is an indication that the Arrhenius law may not describe the physics of the relaxation peak [5,6,23]. It is generally believed that two factors in the nanoparticles will lead to non-Arrhenius law behavior. The first factor is the size distribution, which does not apply to our samples, as it is composed of mono-dispersed particles with a narrow particle distribution. The second factor is the existing dipole–dipole interaction between the particles, which can certainly change the magnetic behavior of a nanoparticle system [7], even leading to a spin-glass behavior in some cases with strong interaction [5,6,24,25]. In our case, it is the second factor is responsible for the unreasonable $v$ value. We are now analyzing our data by considering the effect of interaction.

The dipole–dipole interaction can be estimated [6] by using $E_{d-d}/k_B = (\mu_0/4\pi k_B)M_S^2 V\varepsilon$. With $M_S = 1435\,emu/cm^3$ [26], $V = 3.34\times10^{-26}\,m^3$ and $\varepsilon = 0.3\%$ for our diluted samples, we estimated the interaction is on the order of $E_{d-d}/k_B = 1.5\,K$. The extent of interaction can also be quantified by the Curie–Weiss temperature in the equilibrium susceptibility $\chi_0 = C/(T-\theta)$. As shown earlier, in our diluted samples, $\theta$ is $-5.2\,K$, with the negative sign indicating an antiferromagnetic interaction.

For an interacting systems, Vogel–Fulcher law,

$$\tau = \tau_0 \exp\left[\frac{U}{k_B(T-T_0)}\right], \tag{5}$$

is frequently used to describe the physics of the relaxation peak, where $T_0$ is a measure of the magnitude of interaction. By fitting the values of $T_P$ to Vogel–Fulcher law and taking $T_0 = 5.2\,K$, we obtained $U/k_B = 4.47 \times 10^2 \pm 20\,K$, $\hat{o}_0 = 1.9 \times 10^{-11}\,s$. This value of $\hat{o}_0$ $(= v^{-1})$ is now physically meaningful, and in agreement with those obtained in other particle systems [5]. The value of energy barrier, $U/k_B = 447\,K$, corresponds to an anisotropy constant of $1.85 \times 10^5\,J/m^3$, very close to that obtained for 5 nm Co particles in the magnetic-noise experiment [9]. The fact that the interaction between the particles obtained from the AC susceptibility (5.2 K) is larger than the calculated value (1.5 K) may suggest that the dilute sample is not completely homogeneous and may contain small agglomerates of particles in this sample [5].

Another useful piece of information that can be obtained from the AC susceptibility data is the energy barrier distribution. For a single barrier system, if the frequency range of AC-field is broad enough, the so-called Argand diagram becomes a half-circle [14,27]. It can be shown by rewriting Eqs. (2a) and (2b) as

$$(\chi' - \chi_0)^2 + (\chi'')^2 = r^2, \tag{6}$$

where $\chi_0 = (\chi_T + \chi_s)/2$ and $r^2 = (\chi_T - \chi_s)^2/4$.

If the barrier is independent of temperature, the Argand diagrams measured at different temperatures will collapse into one master curve. If there is a distribution in energy barrier, either due to size distribution or dipole-dipole interactions, the Argand diagrams will deviate from a half-circle [11]. Next we will look at Argand diagrams obtained from our samples. We have performed the AC susceptibility as a function of frequency at different temperatures just below the blocking temperature.

The Argand diagrams obtained at $T = 26$, 27, 28 K are shown in Fig. 3 for Sample Random. The same diagrams obtained at same temperatures for Sample Aligned are almost identical to that for Samples Random except the values of the $\chi_T$ and $\chi_s$. The difference in $\chi_T$ and $\chi_s$ for both samples should be expected. It is evident in Fig. 3 that all the data collapse to a master curve and the Argand diagrams can be fitted to a circle, indicating a narrow distribution in energy barrier in our samples. The non-full–half-circle in Fig. 3 could be due to a non-single barrier property of the system caused either by a narrow distribution in volume [9] or by the interaction discussed above. It could be also due to our frequency range being too narrow.

So far, a perfect full–half-circle Argand diagram has not been observed in nanoparticle systems, due to the energy distribution caused either by size distribution or by dipolar interactions. Although the particles used in this study are already very

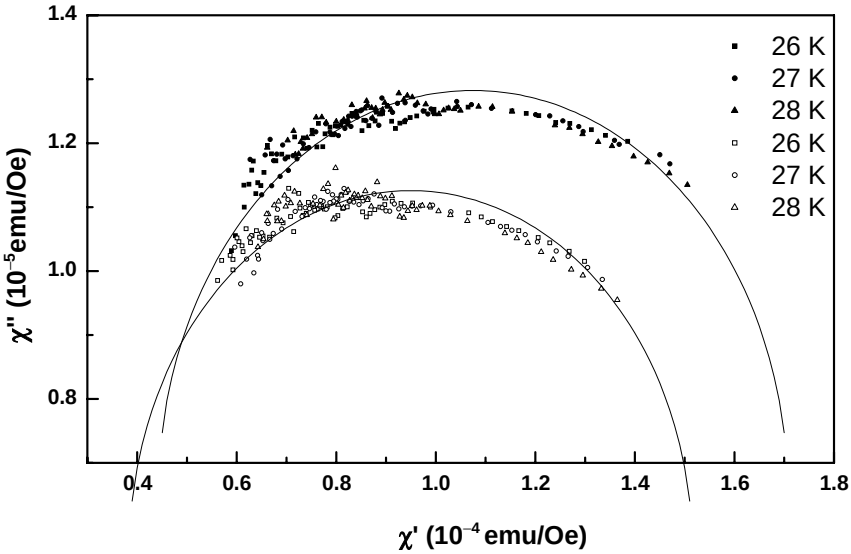


Fig. 3. The Argand diagrams for Co particles. Symbols are the data obtained at different temperatures, Solid (Sample Aligned), Open (Sample Random); the line is the fitted full–half-circle.

uniform and the magnetic fluid is very dilute, there is still some distribution in energy barrier. The only exceptions are the magnetic molecules, e.g. $Mn_{12}$ and $Fe_8$, that show a full–half-circle Argand diagrams [27]. These magnetic molecules represent ideal model systems with a single energy barrier.

Using the same method described above and AC susceptibility data obtained from Sample Aligned, we have also extracted the energy barrier ($U/k_B = 5.2 \times 10^2 \pm 2 \times 10$ K) and the value of ß$_0$ ($\sim 1.9 \times 10^{-11}$ s). The energy barrier is slightly larger than that in the Sample Random. This is because the energy barrier is $KV$ for the aligned particles, whereas for particles with random easy axes, the energy barrier is $\sim KV \cos\phi$ for a particle whose easy axis is at an angle $\phi$ with respect to the applied AC field. The average energy barrier in Sample Random should lower than that in Sample Aligned.

Information on the energy distribution can also be obtained by performing the magnetic relaxation measurements below the blocking temperature. To measure the magnetic relaxation at certain temperature, we first cooled the sample down from 150 K ($\gg T_B$, but it is still low enough to keep the sample to be solid) to the measuring temperature in a field of 500 Oe. We then switched the field to −500 Oe and started to record the time-dependent magnetization. Shown in Fig. 4 are the magnetic relaxation results obtained for the Sample Aligned. It is observed that the time dependent magnetization is well described by the logarithmic decay law,

$$M(t) = M_0 + [M(t_0) - M_0][1 - S\ln(t/t_0)], \qquad (7)$$

where $S = \{1/[M(t_0) - M_0]\}\ \mathrm{d}M/\mathrm{d}(\ln t)$ is the magnetic viscosity. It is well known that magnetic relaxation follows the exponential decay law only when there exists a single barrier in a magnetic particle system,

$$M(t) = M_0 + [M(t) - M_0]\mathrm{e}^{-\Gamma t}, \qquad (8)$$

where $M_0$ is the magnetization associated with the final equilibrium state, $\Gamma = v^{-1}\exp(-U/k_BT)$ is the relaxation rate.

By fitting the relaxation data to Eq. (7), the viscosity and the slope $\mathrm{d}M/\mathrm{dln}\,t$ as a function of temperature are obtained. In the calculation of magnetic viscosity, $M_0$ is chosen as $-M_{FC}$ at the corresponding temperatures, since $M_{FC}$ is a good approximation to the equilibrium magnetization [12]. A careful analysis on the low temperature magnetic viscosity reveals that no plateau is observed down to 1.8 K, in agreement to the

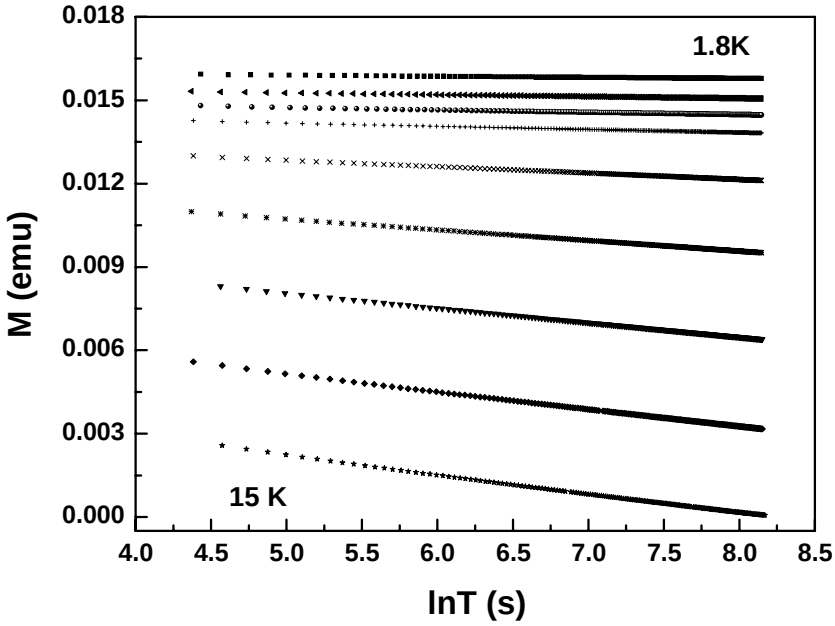


Fig. 4. Time dependent magnetization at different temperatures for Sample Aligned.

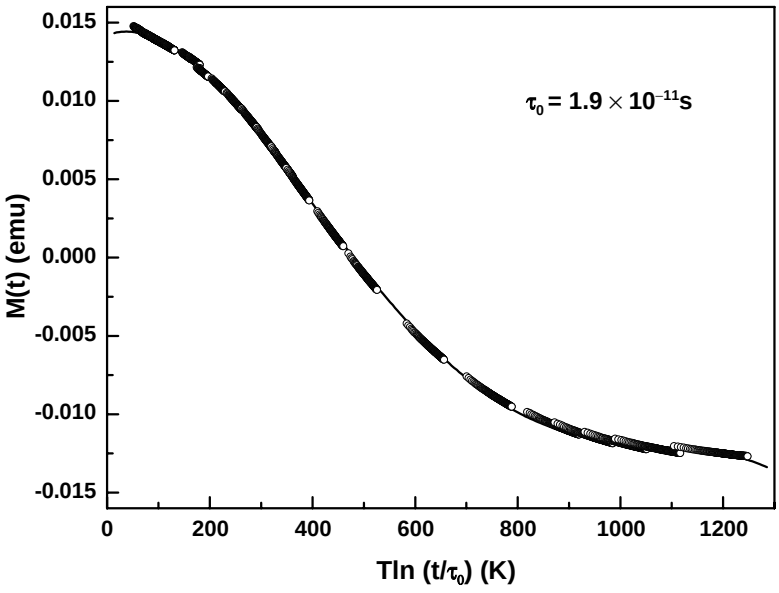


Fig. 5. The time dependent magnetization (relaxation data) scales as a function of $T\ln(t/\tau_0)$.

previous results [11]. Actually, if the relaxation is caused only by thermal effect, all relaxation data can be scaled by $M(t) \sim T\ln(t/\tau_0)$ [8,9,28]. This analysis is based on the fact that most of the magnetization change at temperature $T$ and time $t$ is due to overcoming the barrier of order $U_t = k_B T \ln(t/\tau_0)$, which has been widely used to interpret some aspect of the dynamics of spin glass [29,30] and of random ferromagnets [11,31]. Since this plot consists of relaxation data obtained

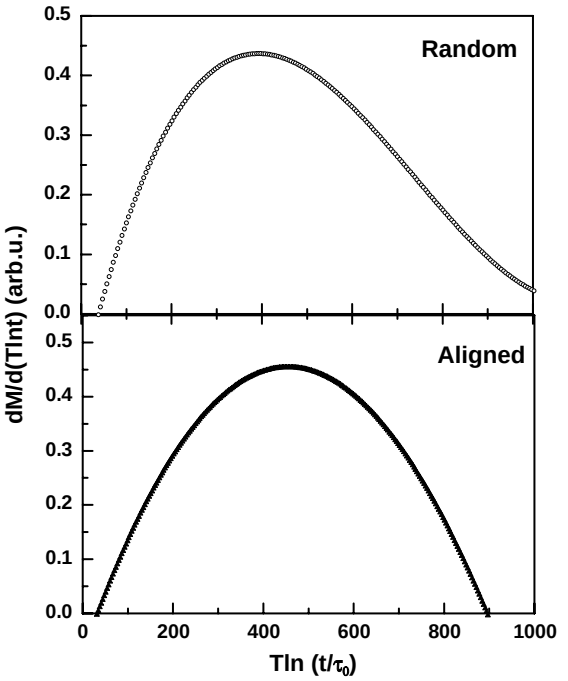


Fig. 6. The lope as a function of $T\ln(t/\tau_0)$, which gives the distribution of energy distribution.

in a wide broad range of temperature and time, the information of whole energy barrier distribution may be obtained from the plot.

It is pointed out by Viencent et al. [12] that the distribution of energy barrier $P(U)$ is proportional to the slope of the curve, $M(t)$ vs. $T\ln(t/\tau_0)$. In our sample, if the distribution is caused by the random distribution of the easy axis, we may try to align the easy axes of the particle using the magnetic field. It is found that the relaxation data obtained from both the Sample Random and Aligned can be plotted against a single variable $T\ln(t/\tau_0)$. Shown in Fig. 5 is the plot of $M(t)$ vs. $T\ln(t/\tau_0)$ for Sample Random. The value of $\tau_0$ is chosen as $1.9\times10^{-11}$ s obtained from both samples. Fig. 6 shows the $dM/d\ln(t/\tau_0)$ vs. $T\ln(t/\tau_0)$. Since the energy barrier distribution $P(U)$ is proportional to the slopes [12], it is clearly seen that the distribution function is modified by the alignment of the easy axes. The distribution becomes more symmetric for the Sample Aligned. This is an interesting experimental observation that the alignment of the easy axes can change distribution of the energy barrier.

In conclusion, hexagonally closely packed self-assembled Co nanocrystals exhibits increased blocking temperature and Curie–Weiss temperature over their diluted counterparts. Our study has shown that magnetic dipolar interaction is significant in concentrated system. Magnetic relaxation models based on single domain particles have been confirmed in all of our Co nanocrystal systems. We have also found that the alignment of easy-axis affects the magnetic relaxation profoundly compared with randomly distributed easy axes. The uniform shape and size of the nanocrystals produced using our method make them potentially good candidates for magnetic recording mediums and magnetic memory devices.

## Acknowledgements

The work described in this paper was partially supported by a grant from the Research Grants Council (RGC) and Industry Support Funds (ISF) of the Hong Kong Special Administration Region, China (HKUST6111/98P, AF/155/99) and partially by the National Science Foundation Grant Nos. DMR-0071770 and DMR-0074080.

## References

[1] C. Petit, T. Cren, D. Roditchev, W. Sacks, J. Klein, M.-P. Pileni, Adv. Mater. 11 (1999) 1198.
[2] C.T. Black, C.B. Murray, R.L. Sandstrom, S. Sun, Science 290 (2000) 1131.
[3] S. Sun, C.B. Murray, D. Weller, L. Folks, A. Moser, Science 287 (2000) 1989.
[4] S. Sun, S. Anders, H.F. Hamann, J.-U. Thiele, J.E.E. Baglin, T. Thomson, E.E. Fullerton, C.B. Murray, B.D. Terris, J. Am. Chem. Soc. 124 (2002) 2884.
[5] C. Djurberg, P. Svedlindh, P. Nordblad, M.F. Hansen, F. Bødker, S. Mørup, Phys. Rev. Lett. 79 (1997) 5154.
[6] T. Jonsson, J. Mattsson, C. Djurberg, F.A. Khan, P. Nordblad, P. Svedlindh, Phys. Rev. Lett. 75 (1995) 4138.
[7] J. García-Otero, M. Porto, J. Rivas, A. Bunde, Phys. Rev. Lett. 84 (2000) 167.
[8] M.R. Diehl, Jae-Young Yu, J.R. Heath, G.A. Held, H. Doyle, Shouheng Sun, C.B. Murray, J. Phys. Chem. B 105 (2001) 7913.

[9] S.I. Woods, J.R. Kirtley, Shouheng Sun, R.H. Koch, Phys. Rev. Lett. 87 (2001) 137 205.
[10] G.A. Held, G. Grinstein, H. Doyle, Shouheng Sun, C.B. Murray, Phys. Rev. B 64 (2001) 012408.
[11] J. Tejada, X.X. Zhang, E.M. Chudnovsky, Phys. Rev. B 47 (1993) 14977.
[12] E. Vincent, J. Hamman, J. Prene, E. Tronc, J. Phys, France 4 (1994) 273.
[13] J.M. González–Miranda, J. Tejada, Phys. Rev. B 49 (1994) 3867.
[14] J.A. Mydoch, Spin Glasses An Experimental Introduction, Taylor & Francis, Washington DC, 1993.
[15] S. Sun, C.B. Murray, J. Appl. Phys. 85 (1999) 4325.
[16] W.A. Sucksmith, J.E. Thompson, Proc. R. Roc. London Ser. A 225 (1954) 362.
[17] D.S. Chuang, C.A. Ballentine, R.C. O'Handley, Phys. Rev. B 49 (1994) 15084.
[18] J.P. Chen, C.M. Sorensen, K.J. Klabunde, G.C. Hadjipanayis, Phys. Rev. B 51 (1995) 11527.
[19] C. Johansson, M. Hanson, P.V. Hendriksen, S. Morup, J. Magn. Magn. Mater. 122 (1993) 125.
[20] S. Linderoth, L. Balcells, A. Labarta, J. Tejada, P.V. Hendriksen, S.A. Sethi, J. Magn. Magn. Mater. 124 (1993) 269.
[21] P. Prene, E. Tronc, J.P. Jolivet, J. Livage, R. Cherkaoui, M. Nogues, J.L. Dormann, D. Fiorani, IEEE Trans. Magn. 29 (1993) 2658.
[22] D.P.E. Dickson, N.M.R. Reid, C. Hunt, J.D. Williams, M. El-Hilo, K. O'Grady, J. Magn. Magn. Mater. 125 (1993) 345.
[23] J.L. Zhang, C. Boyd, Weili Luo, Phys. Rev. Lett. 77(1996) 390.
[24] W. Luo, S.R. Nagel, T.F. Rosenbaum, R.E. Rosensweig, Phys. Rev. Lett. 67 (1991) 2721.
[25] S. Mørup, E. Tronc, Phys. Rev. Lett. 72 (1994) 3278.
[26] B.D. Cullity, Introduction to Magnetic Materials, Addison-Wesley, Reading, MA, 1972.
[27] X.X. Zhang, in: S. H. Yang, P. Sheng (Eds.), Physics and Chemistry of Nano-structured Materials, Taylor and Francis, UK, 2000, p. 176.
[28] A. Labarta, O. Iglesias, L. Balcells, F. Badia, Phys. Rev. B 48 (1993) 10240.
[29] J.J. Prejean, J. Souletie, J. Phys. France 41 (1980) 1335.
[30] R. Omari, J.J. Prejean, J. Souletie, J. Phys. France 45 (1984) 1809.
[31] M. Uehara, B. Barbara, J. Phys. France 47 (1986) 235.